Molecular Control over Semiconductor Surface Electronic Properties: Dicarboxylic Acids on CdTe, CdSe, GaAs, and InP

R. Cohen,[†] L. Kronik,[†] A. Shanzer,[‡] David Cahen,*[,†] A. Liu,[§] Y. Rosenwaks,[§] J. K. Lorenz,[||] and A. B. Ellis[||]

Contribution from the Departments of Materials and Interfaces and of Organic Chemistry, Weizmann Institute of Science, Rehovot 76100, Israel, Department of Physical Electronics, Tel-Aviv University, Ramat-Aviv 69978, Israel, and Department of Chemistry, University of Madison-Wisconsin, Madison, Wisconsin 53706

Received February 26, 1999

Abstract: We present "design rules" for the selection of molecules to achieve electronic control over semiconductor surfaces, using a simple molecular orbital model. The performance of most electronic devices depends critically on their surface electronic properties, i.e., surface band-bending and surface recombination velocity. For semiconductors, these properties depend on the density and energy distribution of surface states. The model is based on a surface state-molecule, HOMO-LUMO-like interaction between molecule and semiconductor. We test it by using a combination of contact potential difference, surface photovoltage spectroscopy, and time- and intensity-resolved photoluminescence measurements. With these, we characterize the interaction of two types of bifunctional dicarboxylic acids, the frontier orbital energy levels of which can be changed systematically, with air-exposed CdTe, CdSe, InP, and GaAs surfaces. The molecules are chemisorbed as monolayers onto the semiconductors. This model explains the widely varying electronic consequences of such interaction and shows them to be determined by the surface state energy position and the strength of the molecule−surface state coupling. The present findings can thus be used as guidelines for molecule-aided surface engineering of semiconductors.

I. Introduction

The performance of most semiconductor-containing devices is critically dependent on the electronic properties of the semiconductor surface, especially the surface band bending (V_s) and the surface recombination velocity (SRV).[1,2] These properties, in turn, depend on the density and energy distribution of surface states.[3] Because the surface state properties are controlled by the chemistry of the surface, much effort has been devoted to developing chemical treatments (both inorganic[4−11] and organic[12−21]) that modify the surface states and hence the surface electronic structure in a desired manner.

Potentially, the use of organic or organometallic molecules as surface treatments holds great promise for fine-tuning the desired surface electronic properties for several reasons. First, a large variety of such molecules are available and new ones can be designed and synthesized. Second, several functional groups can be incorporated in the same molecule. Thus, a group that optimizes molecular binding to the surface can be augmented with auxiliary groups which provide control over molecular dipole moments, frontier orbital energy levels, light sensitization properties, hydrophilic/hydrophobic character, etc. Third, because the electronic properties are controlled by a very thin (and ideally monomolecular) layer, such a layer may potentially be used for fine-tuning *interface* electronic properties without impeding carrier transport through the interface. Indeed, various types of such molecular treatment-induced changes in

[†] Department of Materials and Interfaces, Weizmann Institute of Science.
[‡] Department of Organic Chemistry, Weizmann Institute of Science.
[§] Department of Physical Electronics, Tel-Aviv University.
[||] Department of Chemistry, University of Madison-Wisconsin.

(1) Sze, S. M. *Physics of Semiconductor Devices*, 2nd ed.; John Wiley & Sons: New York, 1981.
(2) Brillson, L. J. *Contacts to Semiconductors*; Noyes Publications: Park Ridge, NJ, 1993.
(3) Many, A.; Goldstein, Y.; Grover, N. B. *Semiconductor Surfaces*; North-Holland: Amsterdam, 1965.
(4) Cahen, D.; Noufi, R. *Appl. Phys. Lett.* **1989**, *54*, 558−560.
(5) Nelson, R. J.; Williams, J. S.; Leamy, H. J.; Miller, B.; Casey, H. C.; Parkinson, B. A.; Heller, A. *Appl. Phys. Lett.* **1980**, *36*, 76−79.
(6) Gayen, S.; Ermler, W. C.; Sandroff, C. J. *J. Phys. Chem.* **1991**, *95*, 7357−7361.
(7) Yablonovitch, E.; Sandroff, C. J.; Bhat, R.; Gmitter, T. *Appl. Phys. Lett.* **1987**, *51*, 439−441.
(8) Fan, J.-F.; Oigawa, H.; Nannichi, Y. *Jpn. J. Appl. Phys.* **1988**, *27*, L1331−L1333.
(9) Troost, D.; Koenders, L.; Fan, L.-Y.; Mönch, W. *J. Vac. Sci. Technol.* **1987**, *B5*, 1119−1124.
(10) Nelson, A. J.; Frigo, S. P.; Rosenberg, R. A. *J. Appl. Phys.* **1994**, *75*, 1632−1637.
(11) Bose, D. N.; Roy, J. N.; Basu, S. *Mater. Lett.* **1984**, *2*, 455−457.
(12) Lunt, S. R.; Ryba, G. N.; Santangelo, P. G.; Lewis, N. S. *J. Appl. Phys.* **1991**, *70*, 7449−7467.
(13) Lisensky, G. C.; Penn, R. L.; Murphy, C. J.; Ellis, A. B. *Science* **1990**, *248*, 840−843.
(14) Murphy, C. J.; Lisensky, G. C.; Leung, L. K.; Kowach, G. R.; Ellis, A. B. *J. Am. Chem. Soc.* **1990**, *112*, 8344−8348 and references therein.
(15) Zhang, J. Z.; Ellis, A. B. *J. Phys. Chem.* **1992**, *96*, 2700−2704 and reference therein.
(16) Lorenz, J. K.; Kuech, T. F.; Ellis, A. B. *Langmuir* **1998**, *14*, 1680−1683.
(17) Lauerhaas, J. M.; Sailor, M. J. *Science* **1993**, *261*, 1567−1568.
(18) Lauerhaas, J. M.; Credo, G. M.; Heinrich, J. L.; Sailor, M. J. *J. Am. Chem. Soc.* **1992**, *114*, 1911−1912.
(19) Asai, K.; Miyashita, T.; Ishigure, K.; Fukatsu, S. *J. Appl. Phys.* **1995**, *77*, 1582−1586.
(20) Lu, E. D.; Zhang, F. P.; Xu, S. H.; Yu, X. J.; Xu, P. S.; Han, Z. F.; Xu, F. Q.; Zhang, X. Y. *Appl. Phys. Lett.* **1996**, *69*, 2282−2284.
(21) Sweryda-Krawiec, B.; Chandler-Henderson, R. R.; Coffer, J. L.; Rho, Y. G.; Pinizzotto, R. F. *J. Phys. Chem.* **1996**, *100*, 13776−13780 and references therein.

10.1021/ja9906150 CCC: $18.00
Published on Web 10/30/1999

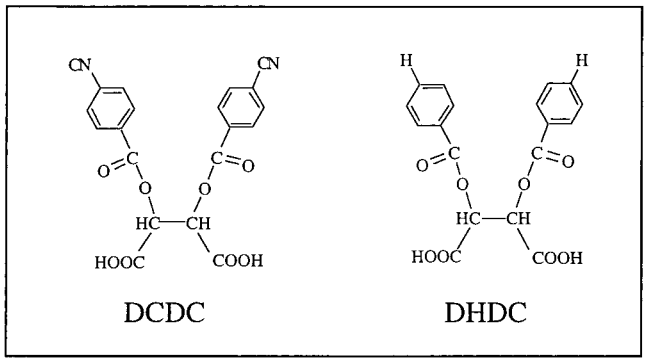

Figure 1. The chemical structure of dicyano dicarboxylic acid (DCDC; right) and dihydrogen dicarboxylic acid (DHDC; left).

V_s and/or SRV have been reported for GaAs,[12,19,20] Si,[18,21,22] CdS,[13,23] and CdSe.[13−16,23,24]

In a preliminary report, the adsorption of a series of dicarboxylic acid derivatives on etched *n*-CdTe surfaces was shown to result in V_s modifications, which varied strongly with the derivative used.[25] These band bending changes were found to stem from two main contributions : a constant contribution due to the binding group and a variable contribution. The latter contribution was correlated with the molecule's lowest unoccupied molecular orbital (LUMO) energy and increased with decreasing energy separation between the molecule's LUMO state and the surface state energy levels. The dependence on the molecular energy level was explained by a semiquantitative model. In this model a LUMO-HOMO (highest occupied molecular orbital) type of interaction between the HOMO-like semiconductor surface states and the molecular LUMO levels can push the former down in energy into the valence band, thereby delocalizing some of the electrons that were trapped in surface states and reducing V_s. The variable effect of the molecular treatment was therefore explained as a result of the variable overlap and interaction between surface states and molecular LUMO levels.

That tentative conclusion was based on results obtained by treating *the same semiconductor surface* with a series of molecules. Naturally, such a model may be semiconductor specific and thus not of general interest. To check the general validity of the model we extended this investigation to several different semiconductors, including *p*-type ones. We chose a specific dicarboxylic acid−dicyano dicarboxylic acid (DCDC), shown in Figure 1, because in the preliminary experiments we found that with this molecule the effect of the orbital interaction on V_s dominates over that of the binding group.[25] In all experiments, a second dicarboxylic acid with a significantly different LUMO level, dihydrogen dicarboxylic acid (DHDC), also shown in Figure 1, was used as a control. We studied the interaction of DCDC and DHDC with several important *n*-type semiconductor surfaces − CdTe(111), CdSe(0001), GaAs(100), and InP(100) − as well as with *p*-GaAs(100). In each case, the effect of the acid on the band bending, gap states, and surface recombination velocity was determined using high-intensity surface photovoltage measurements, surface photovoltage spectroscopy, and time- and intensity-resolved photoluminescence measurements (for CdSe), respectively. These experiments were designed with the purpose of (a) obtaining a comprehensive correlation between semiconductor surface electrical properties and molecular microscopic properties, (b) testing the above-described model, using a much wider set of experimental conditions, involving the interaction of molecular levels with several semiconductor surfaces, and (c) establishing "design rules" for molecule selection, based on the desired surface electronic effect, the surface band diagram, and the molecular orbitals.

II. Molecule−Surface Orbital Interaction Model

Our basic model for describing molecule-induced modifications in semiconductor surface electronic properties relies on an orbital interaction between the molecules and the semiconductor surface states. It is a natural extension of the well-known HOMO-LUMO interaction between the energy levels of two molecules forming a complex, applied to surfaces.[26] This model, shown in the inset of Figure 2, generally leads to a stabilization of the HOMO level and a destabilization of the LUMO level. A qualitative version of it has been used by Ellis and co-workers to explain the molecule-induced changes in the luminescence intensity of *n*-CdSe and *n*-CdS crystals observed upon adsorption of different molecular acids[15] and bases.[14] We formulate it in a way so as to make it generally applicable and to allow its use as a semiquantitative guide to describe semiconductor−molecule interaction. We then demonstrate its validity by presenting clear evidence for molecule-induced shifts of surface states on a series of semiconductors. Despite the consistent nature of the molecule−surface state interaction, its electronic consequences can vary considerably. Therefore, we consider below three prototypical cases.

In the first case, shown in Figure 2a, the surface of an *n*-type semiconductor is in depletion due to filled surface states, which are shallow, i.e., close to the valence band (VB). Upon molecule adsorption, these filled states assume the role of the HOMO levels and interact with the LUMO level of the adsorbed species. Therefore, following the interaction, the surface states are pushed down in energy, i.e., move toward the valence band, and the molecular LUMO level is pushed up, i.e., moves toward the conduction band (CB). After the interaction, part of the surface states are pushed to energies below the VB maximum and become surface resonances.[27] As a result, the main effect of the surface−molecule interaction is a reduction in the surface charge and hence in V_s. This is because electrons that were formerly localized at surface states above the VB maximum are now delocalized in the VB and do not contribute to the surface charge.

As a second case, we consider the complementary scenario to the first case, namely, the surface of a *p*-type semiconductor. This surface is in depletion due to empty surface states which are close to the CB, i.e., shallow (Figure 2b). Because the LUMO level of the molecule is well below the Fermi level, (E_F), electron transfer from the surface to the adsorbate is

(22) Cohen, R.; Zenou, N.; Cahen, D.; Yitzchaik, S. *Chem. Phys. Lett.* **1997**, *279*, 270−274.

(23) Kepler, K. D.; Lisensky, G. C.; Patel, M.; Sigworth, L. A.; Ellis, A. B. *J. Phys. Chem.* **1995**, *99*, 16011−16017.

(24) Neu, D. R.; Olson, J. A.; Ellis, A. B. *J. Phys. Chem.* **1993**, *97*, 5713−5716.

(25) Cohen, R.; Bastide, S.; Cahen, D.; Libman, J.; Shanzer, A.; Rosenwaks, Y. *Adv. Mater.* **1997**, *9*, 746−749.

(26) Hoffman, R. *Solids and Surfaces: A Chemist's View of Bonding in Extended Structures*; VCH: New York, 1988.

(27) Surface resonances are states with energy levels outside the band gap that are degenerate with the bulk states and can mix with them. They have a large amplitude on surface atoms, *compared to bulk states*, i.e., some (varying) degree of localization in the surface region (Lüth, H. *Surfaces and Interfaces of Solid Materials*; Springer, Berlin, 1998. Zangwill, A. *Physics at Surfaces*; Cambridge, 1988. Hansson, G. V., Uhrberg, I. G. Photoelectron Spectroscopy of Surface States on Semiconductor Surfaces. *Surf. Sci. Rep.* **1988**, *9*, 197−292). We note that there is no absolute definition for how strong a surface localization should be, to be defined as a surface resonance.

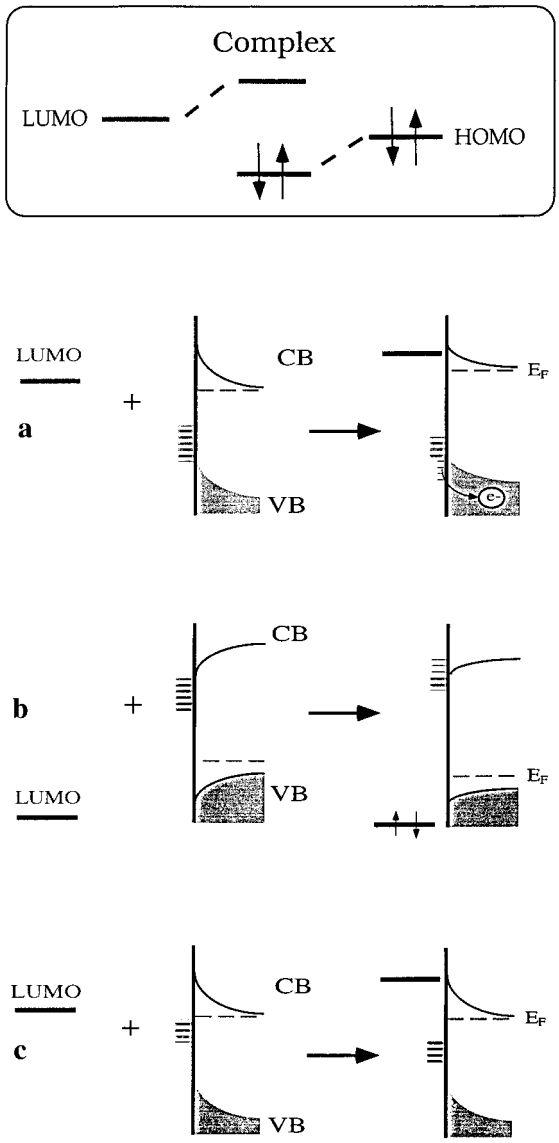

Figure 2. Surface band diagrams for the suggested HOMO-LUMO interaction mechanisms of organic molecules with semiconductor surfaces: (a) shallow filled states, (b) shallow empty states, and (c) deep filled states. Inset: HOMO-LUMO interaction between the energy levels of two molecules forming a complex.

energetically favorable. Therefore, upon interaction, the molecule's LUMO level is expected to become filled with electrons. This means that the surface−molecule interaction is reversed. Upon interaction, the surface states are pushed *up* in energy, i.e., move toward the CB, and the molecular LUMO level is pushed *down*, i.e., moves toward the VB. Consequently, some of the shallow empty states are pushed to energies above the CB minimum, become surface resonances, and do not contribute significantly to the surface charge. If, after adsorption, the LUMO level is below the E_F, this will be an additional cause for V_s reduction, especially if it will act as a surface state (if situated in the band gap) and less so if acting as a surface resonance (if equienergetic with the VB). The reason is that the (partially) localized electronic charge in these states will reduce the net surface (positive) charge, and thus V_s.[28]

As a third case, we consider the molecular interaction with filled *deep* surface states, i.e., states which are closer to midgap, found at a depleted *n*-type semiconductor (Figure 2c). As in the first case (Figure 2a), we expect the interaction to push the surface states downward in energy. However, in contrast to the first case, because the surface states are initially away from the VB, only a small portion of them will become surface resonances and the total surface state density inside the band gap will not be altered significantly. Hence, V_s, will remain approximately the same. Here, the molecular interaction is chiefly expected to affect the SRV. This is because the latter is typically dictated by deep surface states.[29] Whether the SRV will increase or decrease depends on whether the surface states are, on average, pushed toward midgap or away from midgap, respectively.

It is important to note that Figure 2 represents three *extreme* cases. Clearly, the extent of the surface state energy modification depends on the strength of the molecule−surface state orbital coupling. The latter is generally expected to increase with decreasing energy separation between the HOMO and LUMO levels. It is also expected to vary with orbital shape, e.g., due to symmetry considerations. Moreover, the semiconductor surface may possess several populations of surface states. Practical cases may therefore feature elements of more than one of the scenarios depicted above.

We further note that scenarios similar to those illustrated in Figure 2, involving, e.g., empty states on an *n*-type surface or filled states on a *p*-type surface, can be constructed by analogy. Such analogies further tell us that one can also consider, e.g., interaction between the HOMO level of the molecule and empty surface states. The latter case is not considered further in this work because the HOMO levels of the molecules studied are several electron volts (eV) below those of the surface states, so that any potential interaction is negligible.

III. Experimental Section

Strategy. To test the above-presented model, the pertinent surface electronic parameters, namely V_s and the SRV, were measured both before and after adsorption of dicarboxylic acids, using complementary experimental approaches.

A lower limit to the surface band-bending, V_{ps} ($|V_{ps}| \leq |V_s|$), was found using the photosaturation (ps) technique.[30] This technique is based on the fact that the surface band bending is significantly reduced, and ideally nullified, under intense illumination. Therefore, the band bending is estimated as the surface photovoltage (=photoinduced change in surface band-bending) under intense illumination. The SRV was extracted by fitting picosecond time-resolved photoluminescence (TRPL) decay curves. Mathematical details of the fitting procedure have been published elsewhere.[31] Additionally, intensity-resolved photoluminescence (PL) measurements at several wavelengths were used to confirm the changes in V_s and SRV of CdSe samples. In this method,[13,32] modifications in V_s are revealed by considering modifications in the dead layer, which is a nonemissive layer near the surface. This layer is assumed to be of the order of the depletion region, but not strictly equal to it.[14,33] If the dead layer model is applicable, then the relation $PL_{bare}(\lambda)/PL_{mol}(\lambda) = \exp(-\alpha'(\lambda)\Delta D)$ should hold, irrespective of wavelength (shorter than the absorption edge). Here PL_{bare} and

(28) We thank a reviewer for pointing this consequence of the model out to us. In this case, electrons that were delocalized in the band continuum will, upon molecule adsorption, become (partially) localized on the surface. This leads to a positive countercharge near the surface. The resulting electrical potential difference will reduce V_s. The opposite effect occurs with n-type material, where one starts with electrons, localized in filled surface states, which, upon molecule adsorption, are partially delocalized in the VB.

(29) Lang, D. V.; Henry, C. H. *Phys. Rev. Lett.* **1975**, *35*, 1525−1528.
(30) Aphek, O. B.; Kronik, L.; Leibovitch, M.; Shapira, Y. *Surf. Sci.* **1998**, *409*, 485−500.
(31) Rosenwaks, Y.; Thacker, B. R.; Nozik, A. J.; Shapira, Y.; Huppert, D. *J. Phys. Chem.* **1993**, *97*, 10421−10429.
(32) Ellis, A. B.; Brainard, R. J.; Kepler, K. D.; Moore, D. E.; Winder, E. J.; Kuech, T. F.; Lisensky, G. C. *J. Chem. Educ.* **1997**, *74*, 680−684.
(33) Hollingsworth, R. E.; Sites, J. R. *J. Appl. Phys.* **1982**, *53*, 5357−5358.

PL_{mol} are the PL intensity for the bare and molecule-adsorbed surface, respectively, α' is the sum of the semiconductor absorption coefficients for the exciting and emitted light, and ΔD is the adsorption-induced difference in the dead layer thickness.

The SRV and V_s changes were correlated with changes in the surface state positions relative to the band edges. The latter were extracted from surface photovoltage spectroscopy (SPS) measurements. In SPS, sharp slope changes in the surface photovoltage vs photon energy curves, at sub-band gap photon energies, are attributed to the onset of electron transitions between surface states and band edges.[34−36] A *negative* change in slope implies electron excitation from a filled surface state to the CB minimum, whereas a *positive* change in slope implies electron excitation from the VB maximum to an unoccupied surface state. At the band gap energy, another sharp slope change indicates the onset of super-band gap absorption, which reduces V_s. A negative slope change indicates a surface depletion layer of an *n*-type material (bands bent upward toward the surface), whereas a positive slope change indicates a surface depletion layer of a *p*-type material (bands bent downward toward the surface).

Finally, the position of the surface states with respect to the vacuum level was estimated by combining the photosaturation and surface photovoltage (SPV) data with direct measurements of the surface work function, obtained via the Kelvin probe technique.[36] This allowed us to estimate the surface state positions with respect to the positions of the DCDC and DHDC LUMO levels quantitatively.

Materials. Unintentionally *p*-doped (specific resistivity: 30 Ω·cm) CdTe(111) single crystals were obtained from II-VI Inc., USA, and were In-doped to $n = (1-5) \times 10^{17}$. Details of the doping procedure have been published elsewhere.[37] The results of various measurements performed on *n*-CdTe differed significantly between two different manufacturing batches, even though these two batches were processed and measured under the same conditions. These two variations are referred to below as "type I" and "type II". All other crystals were *p*- or *n*-doped as purchased. These included the following: *n*-CdSe(0001) (7×10^{15} cm^{-3}, Cleveland Crystals, USA); *n*-GaAs(100) (3×10^{18} cm^{-3}, AXT, USA); *n*-InP(100) (4×10^{16} cm^{-3}, Crystacomm, USA); and *p*-GaAs(100) (2×10^{17} cm^{-3}, ITME, Poland).

Surface Treatments. CdTe and CdSe samples were first mechanically polished with a 0.05 μm alumina suspension, whereas no such polishing was required for the GaAs and InP samples. All samples were subsequently etched chemically. Etching procedures of the CdTe, CdSe, and GaAs surfaces are described in refs 38−40, respectively. InP surfaces were etched according to the GaAs procedure. All etching treatments were performed on freshly cut substrates. Back (Ohmic) contacts to the samples were obtained using a eutectic (In,Ga) alloy. Chemisorption of the dicarboxylic acids was performed immediately after etching by overnight immersion of the samples in a 2.5 mM molecular solution in acetonitrile (HPLC and spectroscopic grade). The samples were then rinsed with a pure acetonitrile solution for 10 s to remove excess unbound molecules, resulting in a surface coverage of about one monolayer, verified by FTIR.[41−43] Longer or additional acetonitrile rinse did not change the surface coverage.

Using adsorption isotherms derived from FTIR spectra and from special electrical measurements, Vilan et al. found binding of DCDC and DHDC onto GaAs(100) to be best described by a two-site process, with binding constants of 3×10^6 and 3×10^5 M^{-1}, respectively.[43,44] These values are higher than those of benzoic acids onto the same surface ($\sim 2 \times 10^4$ M^{-1})[40] or onto CdTe (1.3×10^3 M^{-1}),[45] for processes best described by a one-site process.

For the dicarboxylic acids used here the FTIR spectra did not reveal any spectral differences between adsorption of DHDC and DCDC. We can speculate that the difference in the binding constant between DCDC and DHDC is related to the strength of the orbital coupling with the surface states and, thus, correlated with changes in V_s. However, more information is needed to verify this issue.

Opto-Electronic Measurements. The semiconductor surface work function was determined in a contactless, nondestructive manner by CPD measurements, using a Kelvin probe arrangement (Delta-Phi Elektronik).[36] The CPD is defined as the work function difference between the sample surface and an inert reference electrode, in this case made of Au and with a known work function of 5.1 eV. All measurements were conducted in the ambient inside a homemade Faraday cage. Surface photovoltages were determined by photoinduced changes in the CPD.

High-intensity white illumination of $\sim$200 mW/cm^2 was obtained from a quartz tungsten−halogen lamp for the photosaturation experiments. For SPS measurements, monochromatic illumination was generated by passing light from a 600 W quartz tungsten−halogen lamp (Oriel) through a grating monochromator (Model 270M, Jobin Yvon) and an automated filter wheel (Model AB300, CVI) and focusing it on the sample. Because the SPV induced by super-band gap illumination was very large with respect to that induced by sub-band gap illumination, a strong attenuation of the second-order intensity of the monochromator was required. Optical filters were therefore chosen such that the second-order attenuation was at least 10 orders of magnitude. The photon energy range was 0.6−2.0 eV (i.e., from sub-band gap to super-band gap energies). The illumination intensity on the sample was lower than 20 μW/cm^2, guaranteeing a low injection level at all photon energies. Due to sample sensitivity to intensity variations, noted experimentally after replacements of gratings and filters, SPV spectra were taken using a constant photon flux (except for the CdTe samples). The constant photon flux was obtained by using a pyroelectric photodetector as the input of a computerized feedback loop that regulated the voltage supply to the lamp at each wavelength.

In some of the samples, the output of the constant photon flux setup was of too low an intensity to observe sub-band gap transitions. In those cases, a second SPS scan without a constant photon flux was performed over the pertinent range of sub-band gap energies, where a further increase of the illumination intensity was achieved by placing a condensing lens before the sample.

Time-resolved photoluminescence measurements were performed using the time-correlated single photon counting technique. The excitation source was a Ti-Sapphire laser (Tsunami, Spectra Physics Inc.) with an excitation wavelength of 730 nm (beam diameter: 1 mm; pulse energy: 5.5 nJ; pulse duration: 1.2 ps). For CdSe, an excitation wavelength of 386 nm (pulse energy: 0. 2 nJ), obtained by frequency doubling the fundamental laser output, was used. The detection system is based on a double subtractive monochromator (CM112, CVI) and an MCP-Photomultiplier (R3809, Hamamatsu). Detection wavelengths for the different semiconductors were 720, 920, and 870 nm for CdSe, InP, and GaAs, respectively. The TRPL measurements for the CdTe crystals were performed using a Nd:YAG pumped dye laser (excitation wavelength: 600 nm; beam diameter: 1 mm; pulse energy: 2 nJ; pulse duration: 1−2 ps). The detection wavelength was 820 nm. More details on the experimental setup have been given elsewhere.[46,47]

Intensity-resolved PL measurements were performed in a nitrogen atmosphere using either a HeNe (Model 80, Melles-Griot) or an Ar^+ (Innova 90, Coherent) laser, with excitation wavelengths of 633 (HeNe), 514 (Ar^+), and 458 nm (Ar^+). The PL signal of CdSe at 720 nm was collected by a CCD array (Instaspec II, Oriel).

(34) Gatos, H. C.; Lagowski, J. *J. Vac. Sci. Technol.* **1973**, *10*, 130−135.
(35) Lagowski, J. *Surf. Sci.* **1994**, *299/300*, 92−101.
(36) Kronik, L.; Shapira, Y. *Surf. Sci. Rep.* In press.
(37) Lyahovitskaya, V.; Kaplan, L.; Goswami, J.; Cahen, D. *J. Cryst. Growth* **1999**, *197*, 106−112.
(38) Bruening, M.; Moons, E.; Yaron-Marcovich, D.; Cahen, D.; Libman, J.; Shanzer, A. *J. Am. Chem. Soc.* **1994**, *116*, 2972−2977.
(39) Bruening, M.; Moons, E.; Cahen, D.; Shanzer, A. *J. Phys. Chem.* **1995**, *99*, 8368−8373.
(40) Bastide, S.; Butruille, R.; Cahen, D.; Dutta, A.; Libman, J.; Shanzer, A.; Sun, L.; Vilan, A. *J. Phys. Chem.* **1997**, *101*, 2678−2684.
(41) Cohen, R.; Bastide, S.; Cahen, D.; Libman, J.; Shanzer, A.; Rosenwaks, Y. *Opt. Mater.* **1998**, *9*, 394−400.
(42) Bastide, S. Unpublished results, Weizmann Institute of Science.
(43) Vilan, A. Chemical Modifcation of the electronic Properties of GaAs Surface. M. Sc. thesis, Weizmann Institute of Science, Rehovot, 1996.
(44) Vilan, A.; Ussyshkin, R.; Gartsman, K.; Cahen, D.; Naaman, R.; Shanzer, A. *J. Phys. Chem. B* **1998**, *102*, 3307−3309.
(45) Yaron-Marcovich, D. Studies of the Adsporption Mechanism of Polar Ligands on the Surface of Chalcogenide Semiconductors. M. Sc. thesis, Weizmann Institute of Science, Rehovot, 1993.
(46) Liu, A.; Rosenwaks, Y. Submitted for publication.
(47) Rosenwaks, Y.; Shapira, Y.; Huppert, D. *Phys. Rev. B* **1991**, *45*, 9108−9119.

Table 1. Summary of Surface Band Bending (V_s) and Surface Recombination Velocity (SRV) of the Different Semiconductor Surfaces before and after Molecule Adsorption

	V_{ps} [mV]			SRV [cm/s]		
crystal	bare	DCDC	DHDC	bare	DCDC	DHDC
n-CdTe (type I)	610 ± 30	110 ± 20	460 ± 10	$(1-3) \times 10^3$	$(1-3) \times 10^3$	$(1-3) \times 10^3$
n-CdTe (type II)	510 ± 30	410 ± 30		$>10^6$	$>10^6$	$>10^6$
n-CdSe	530 ± 30	480 ± 30	520 ± 30	<100	$>10^6$	$>10^6$
n-GaAs	580 ± 60	440 ± 30	490 ± 30	1×10^4	2×10^4	1×10^4
n-InP	470 ± 30	480 ± 40	460 ± 20	<100	$(4-5) \times 10^3$	<100
p-GaAs	220 ± 20	150 ± 30	210 ± 20	$>10^6$	$>10^6$	$>10^6$

Synthesis. A solution of L-tartaric acid (10 g, 0.06 mole) was dissolved in dry $CHCl_3$ and treated with *p*-toluenesulfonic acid monohydrate (13 g, 0.07 mol) and benzyl alcohol (70 mL, 0.7 mol). The reaction mixture was refluxed with a Dyn-stark attached overnight. The solvent was evaporated and the excess of benzyl alcohol was washed several times with hexane. The residue was chromatographed using hexane−ethyl acetate (7:3) to obtain the benzylated tartaric acid (22%): IR ($CHCl_3$) ν (COOBn) 1745 cm^{-1}; ^1H NMR (270 MHz, $CDCl_3$) δ 7.36 (s, 5H, ArH), 5.27 (d, 2H,CH_2Ph, $J = 2.8$ Hz), 4.61 (s, 1H,C*H*(OH)). The benzylated tartaric acid was dissolved in a minimal amount of pyridine and treated under cooling in an ice bath with stoichiometric amounts of the desired alkyloyl chlorides (e.g., *p*-cyanobenzoyl chloride or benzoyl chloride) that was dissolved in $CHCl_3$. The mixture was stirred overnight at room temperature. Then $CHCl_3$ was added and the organic phase was washed with aqueous 1 N HCl, H_2O, 1 N $NaHCO_3$, and again with H_2O, dried with $MgSO_4$, and concentrated in vacuo.

The benzylated derivative of compound DCDC was purified by chromatography using CH_2Cl_2−hexane (6:4) as eluents (yield, 20%): IR ($CHCl_3$) ν (COOR) 1766 cm^{-1}, ν (COOBn) 1725 cm^{-1}; ^1H NMR (270 MHz, $CDCl_3$) δ 7.97 (d, 2H, ArH), 7.19 (m, 5H, Bn), 7.11 (m, 2H, ArH), 6.01 (s, 1H, CHO), 5.20 (d, 2H, CH_2Bn), 3.88 (s, 3H, OCH_3).

The benzyl group (Bn) of DCDC was removed by hydrogenolysis. The benzylated compound (630 mg, 10^{-3} mol) was dissolved in dioxane (60 mL) and was treated with 10% Pd/C (250 mg). The reaction mixture was hydrogenolated for 3 h at atmospheric pressure. The suspension was filtered, washed with dioxane, and concentrated. The crude product was chromatographed using ethyl acetate−ethanol (9:1) as eluents, yielding DCDC (30% yield): mp 186−190 °C; IR (KBr) ν (COOH) 1709 cm^{-1}, ν (C═C) 1609 cm^{-1}; ^1H NMR (400 MHz, MeOD) δ 7.9 (d, 2H, ArH), 6.90 (d, 2H, ArH), 5.79 (s, 1H, CHO), 3.83 (s, 3H, OCH_3).

The benzylated derivative of the compound DHDC was purified by chromatography using $CHCl_3$−hexane (9:1) as eluents: IR ($CHCl_3$) ν (COOR) 1767 cm^{-1}, ν (COOBn) 1732 cm^{-1}; ^1H NMR (400 MHz, $CDCl_3$) δ 7.98 (d, 2H, ArH, $J = 8.4$ Hz), 7.59 (t, 1H, ArH), 7.42 (t, 2H, ArH, $J = 8.0$ Hz), 7.19 (m, 2H, Bn), 7.10 (m, 3H, Bn), 6.01 (s, 1H, CHO), 5.23 (d, 1H, CH_2Bn, $J = 12.1$ Hz), 5.10 (d, 1H, CH_2Bn, $J = 12.1$ Hz).

The benzyl group (Bn) of DHDC was removed by hydrogenolysis. The benzylated compound (1.58 g, 4.4×10^{-3} mol) was dissolved in ethanol absolute (100 mL) and treated with 10% Pd/C (500 mg). The reaction mixture was hydrogenolated for 3 h at atmospheric pressure. The suspension was filtered, washed with dioxane, and concentrated. The crude product was chromatographed using ethyl acetate−ethanol (9:1) as eluents, yielding DHDC (30% yield): IR (KBr) ν (COOH) 1732 cm^{-1}; ^1H NMR (400 MHz, $CDCl_3$) δ 8.04 (d, 2H, ArH, $J = 8.0$ Hz), 7.57 (t, 1H, ArH), 7.42 (t, 2H, ArH, $J = 7.9$ Hz), 5.98 (s, 1H, CHO).

IV. Results and Discussion

V_{ps} and SRV values for all semiconductor surfaces studied, before and after adsorption of DCDC and DHDC, are given in Table 1.[48] By using the surface work function values obtained from CPD measurements in the dark in conjunction with V_{ps} values, approximate surface band diagrams of the semiconductor surfaces were constructed. These are shown in Figure 3a,b for three representative free and DCDC-adsorbed surfaces, respectively: *n*-CdTe(111), *p*-GaAs(100), and *n*-CdSe(0001). The Fermi level position was taken as the average of several measurements with an error of about ±30 mV. The distance between the CB in the bulk and the Fermi level was calculated from the doping density. The surface band bending was estimated from photosaturation measurements. The diagrams were put on a common scale, which also shows the DCDC and DHDC LUMO levels, found as described in ref 25. For facilitating comparison to the theoretical model, the surface band diagrams of Figure 3 also show the approximate surface state energy positions. Those were deduced from SPV spectra, which are discussed in detail below.

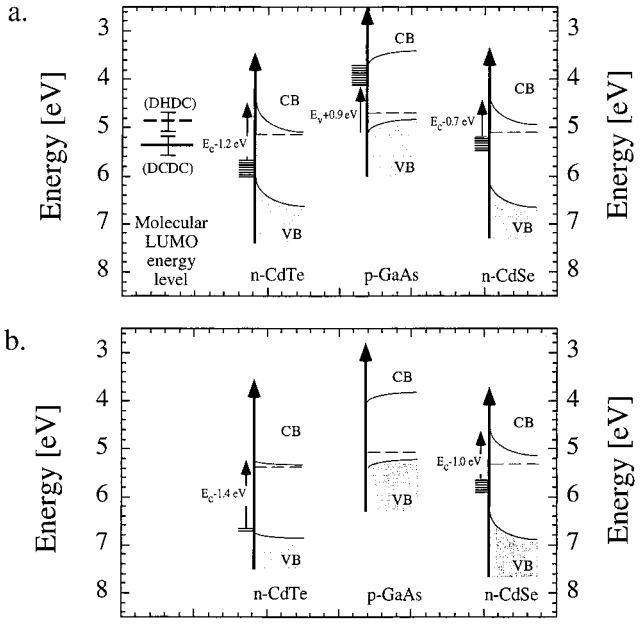

Figure 3. Approximate surface band diagrams of type I *n*-CdTe(111), *p*-GaAs(100), and *n*-CdSe(0001) surfaces, with respect to the DCDC (solid line) and DHDC (dashed line) LUMO level before (a) and after (b) DCDC adsorption. The LUMO level of the molecules is shown before adsorption.

We note that by combining the photosaturation data with CPD measurements in the dark, before and after adsorption of DCDC and DHDC, we found that the adsorbed molecules increased the effective electron affinity of all samples studied. This effect is due to the net dipole moment of the molecules. Indeed, the increase in affinity was larger for DCDC, known to have a larger molecular dipole than for DHDC. Because these dipole effects have been investigated extensively elsewhere[25] they are not discussed further here.

Based on the experimental data, we now turn to a detailed presentation of the experimental results pertinent to each surface

(48) Since the experiments in this work where done in the ambient, formation of surface oxides was unavoidable. Thus, the surface states here are of the bare semiconductor/oxide system before molecule adsorption.

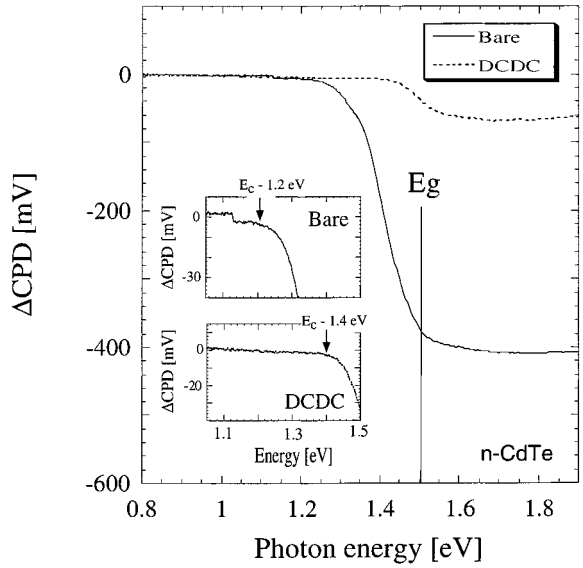

Figure 4. SPV spectra of the (type I) *n*-CdTe(111) surface, before and after DCDC adsorption. Inset: Detailed spectra of the near-band gap photon energy range.

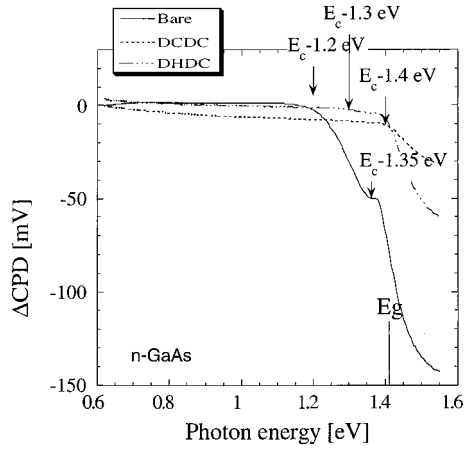

Figure 5. SPV spectra of the bare, DCDC-adsorbed, and DHDC-adsorbed *n*-GaAs(100) surface.

and to their analysis in light of the above-presented model. This analysis is followed by an overview of the common trends found.

Interaction with Shallow Filled States. Using Table 1, we find that at both (type I) *n*-CdTe(111) and *n*-GaAs(100) surface DCDC adsorption causes a significant decrease in V_s, but no significant change in the SRV. This is in complete agreement with the predictions of our model regarding molecular interaction with shallow filled states, i.e., the prototypical case of Figure 2a. We therefore examine whether the rest of our measurements on these surfaces are also in agreement with this prototypical case.

We start with the type I *n*-CdTe(111) surface. SPV spectra of this surface, before and after DCDC adsorption, are presented in Figure 4. The sharp CPD change at ~1.5 eV, present both before and after DCDC adsorption, corresponds to the band gap energy, E_g, of CdTe. Its negative sign indicates an *n*-type crystal, as expected. The magnitude of the SPV signal is expected to decrease with decreasing band bending.[36] Therefore, its reduction following DCDC adsorption is consistent with the reduction in band bending, that is observed in the photosaturation experiment.

The sub-band gap sharp CPD slope change at ~1.2 eV, found before DCDC adsorption, is due to excitation of electrons from a shallow, filled surface state to the conduction band. After DCDC adsorption, the CPD slope change is shifted to ~1.4 eV, indicating that the filled, shallow state is pushed down in energy (i.e., stabilized) by ~0.2 eV.

It should be noted that, *in principle*, a reduction in V_s could cause a shift in the energy position of the sub-band gap knee even if the sub-band gap states are not altered. First, the reduction in V_s reduces the overall SPV signal. Therefore, the threshold above which the SPV signal does not "drown" in the noise level, which is fixed, is shifted to higher energies.[36] However, the magnitude of the super-band gap SPV signal is (approximately) inversely proportional to the square root of V_s.[36,49] Therefore, a 6-fold decrease in V_s, as observed for *n*-CdTe type I (see Table 1), would reduce the sub-band gap SPV by a factor of 2−3 at most. Using Figure 4 and given a ~2 mV noise level, it is readily observed that the DCDC-induced threshold shift is much larger than that anticipated based on this effect. Second, some of the near-band gap absorption (and hence SPV signal) may be due to field-assisted tunneling (known as the Franz−Keldysh effect), rather than due to absorption in sub-band gap states.[36] This absorption also decreases with decreasing V_s. However, the magnitude of the surface electric field is also inversely proportional to the square root of V_s and a reduction by less than half an order of magnitude in this electric field cannot account for an absorption shift of ~200 meV (see Figure 4). Thus, we positively conclude that the SPV threshold genuinely reflects a shift in the position of the surface states and is *not* a misinterpretation of the SPS data.

The observed stabilization of the filled shallow states is in complete agreement with the prototypical case of Figure 2a. Using Figure 3a, we find that prior to adsorption the DCDC LUMO level is at a higher energy than the surface states. Therefore, these states assume the role of HOMO levels and should indeed be stabilized upon interaction. This stabilization pushes some of the filled states into the VB. As a result, the net surface charge is reduced, and so is V_s, as shown in Figure 3b.

Additional support for the model is given by the fact that DHDC adsorption only reduced the band bending by ~150 meV, compared with ~500 meV for DCDC adsorption (see Table 1). This is consistent with the LUMO−surface state energy separation being larger for DHDC than for DCDC (see Figure 3). The increased separation reduces the overall molecule−surface state coupling and therefore the surface state stabilization is less effective. Accordingly, no significant DHDC-induced changes were found in the SPV spectrum either.

We now consider the *n*-GaAs(100) surface. SPV spectra of the bare, DCDC-adsorbed, and DHDC-adsorbed surfaces are presented in Figure 5. The sharp CPD change at ~1.4 eV, present before and after molecule adsorption, corresponds to the GaAs band gap energy. Its negative sign indicates an *n*-type crystal, as expected. Before molecule adsorption, a sharp sub-band gap CPD slope change at ~1.2 eV indicates excitation of electrons from a shallow filled surface state to the conduction band. DCDC and DHDC adsorption shifts this slope change to higher energies by ~0.2 and ~0.1 eV, respectively, indicating a stabilization of the filled surface states.

As in the CdTe surface, and for the same reasons, the observed filled state stabilization is in complete agreement with the prototypical case of Figure 2a. Moreover, here we find direct evidence that the surface state stabilization is more pronounced

(49) Burstein, L.; Bregman, J.; Shapira, Y. *J. Appl. Phys.* **1991**, *69*, 2312−2316.

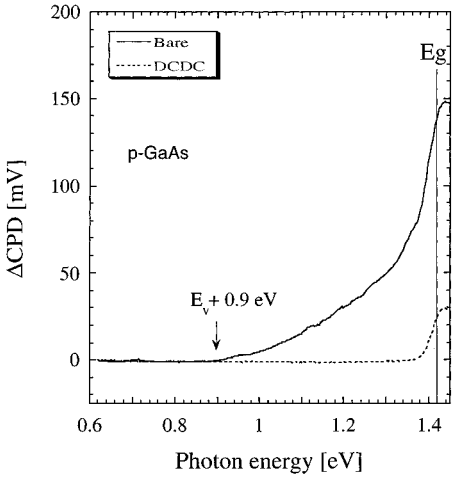

Figure 6. SPV spectra of the *p*-GaAs(100) surface, before and after DCDC adsorption.

with DCDC than with DHDC, in agreement with the larger LUMO−surface states energy separation in the latter. Thus, the *n*-GaAs results lend further support to our model.

Interaction with Shallow Empty States. Using Table 1, we find that DCDC adsorption reduces the band bending at the *p*-GaAs(100) surface. As this is the expected result for the prototypical case of molecule−empty state interaction shown in Figure 2b, we examine whether the rest of our measurements on this surface are in agreement with the prototypical case.

SPV spectra of the bare and DCDC-adsorbed *p*-GaAs(100) surface are presented in Figure 6. As in *n*-type GaAs, the sharp CPD change at ∼1.4 eV, present both before and after DCDC adsorption, corresponds to the band gap energy of GaAs. However, here the sharp CPD change is positive, indicating the *p*-type nature of the sample. As before, the reduction in the magnitude of the SPV signal upon DCDC adsorption supports the photosaturation observation of a reduction in band bending.

The most striking change in the SPV spectra, brought about by DCDC adsorption, is the disappearance of a rather significant sub-band gap signal with an onset at ∼0.9 eV. The positive SPV change at ∼0.9 eV indicates that the signal is due to excitation of electrons from the VB into empty surface states located ∼0.9 eV above the VB. While states located ∼0.5 eV below the CB minimum are not truly "shallow" in the traditional sense, the SPV spectra clearly show that they are destabilized upon DCDC adsorption, as no sub-band gap signal is apparent until ∼0.1 eV below the band gap energy.

The observed destabilization of the empty states is in agreement with the prototypical case of Figure 2b: using Figure 3a, we find that prior to adsorption the DCDC LUMO level is at a lower energy than the *p*-GaAs surface Fermi level and can be filled upon adsorption. Therefore, this level can assume the role of the HOMO, whereas the empty surface state can assume the role of the LUMO levels in the interaction. The destabilization of the latter pushes some of the states into the CB, the net surface charge is reduced, and so is V_s, as shown in Figure 3b. While the decrease in V_s could also stem from (partial) localization of negative charge in the LUMO of the adsorbed molecule, via formation of surface (resonance) states (near) in the VB, we could not find experimental evidence for this. Further support for our model stems from the fact that while DCDC adsorption reduced the band bending by over 30%, DHDC adsorption did not alter the band bending, within experimental error. This agrees with the position of the DHDC LUMO level, which is close to the Fermi level, as shown in Figure 3a. This level should not fill with electrons upon interaction, and therefore cannot assume the role of a HOMO level and destabilize the empty surface states.

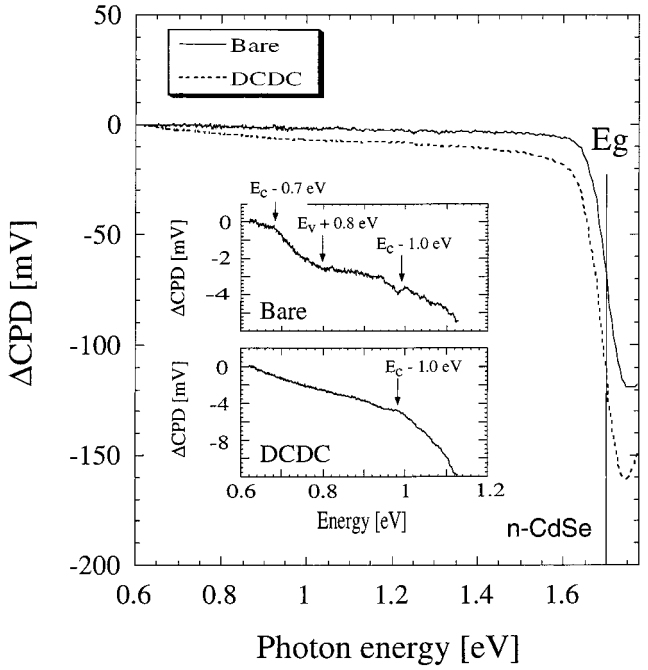

Figure 7. SPV spectra of the *n*-CdSe(0001) surface, before and after DCDC adsorption. Inset: Detailed spectra of part of the sub-band gap photon energy range.

Interaction with Deep States. Using Table 1, we find that at both the *n*-CdSe(0001) and the *n*-InP(100) surfaces DCDC adsorption induces a distinct increase in SRV, but no significant changes in V_s. This agrees with the predictions of the model regarding molecular interaction with deep surface states, i.e., the prototypical case of Figure 2c. We therefore examine if our other measurements on these surfaces are also in agreement with this prototypical case.

We start with the *n*-CdSe(0001) surface. First, as a very large increase in the SRV was obtained, we set out to corroborate the photosaturation and TRPL data of Table 1 with independent intensity-resolved PL measurements. The latter indicated a decrease of the PL intensity upon DCDC adsorption. Such a decrease could, in principle, be understood in terms of an increase of the space charge region width (resulting from an increase in the negative charge held in surface states) from a modification of the SRV or using a combination of both. By relating the calculated change in the dead layer width, ΔD, and the excitation wavelengths we found that the decrease in PL intensity does not fit the dead layer model and hence cannot be attributed predominantly to an increase in the depletion width. These PL results support the notion that DCDC adsorption is accompanied by a substantial change in SRV, in agreement with the data of Table 1.

SPV spectra of this surface, before and after DCDC adsorption, are presented in Figure 7. The sharp CPD change at ∼1.7 eV, present both before and after DCDC adsorption, corresponds to the CdSe band gap energy. Its negative sign indicates an *n*-type crystal, as expected. The magnitude of the SPV signal is not changed appreciably, further indicating that there is no significant change in band bending.

As opposed to all previous spectra, here neither do we find a significant SPV tail due to surface states near one of the bands nor do we see a shift of this tail upon DCDC adsorption. This means that here there is no significant molecular interaction

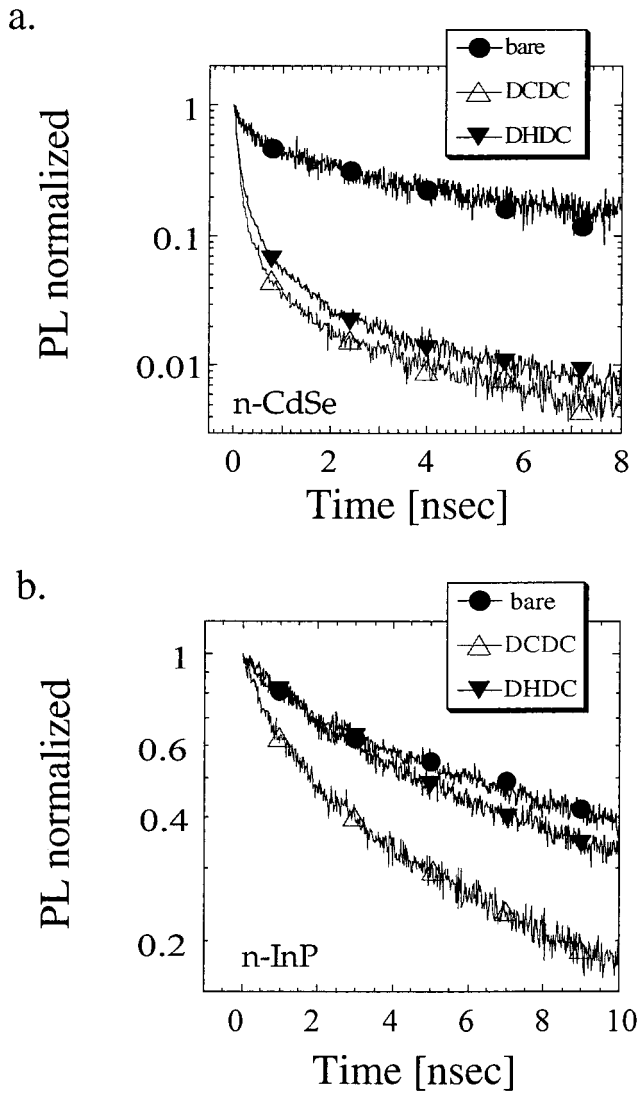

Figure 8. Photoluminescence decay curves of the bare, DCDC-adsorbed, and DHDC-adsorbed surfaces of (a) *n*-CdSe(0001) and (b) *n*-InP(001).

with shallow surface states, which explains the relatively minor changes in the band bending, in agreement with the prototypical case of Figure 2c. On the other hand, a downshift in the surface state energy position, i.e., a stabilization of surface states, is apparent near midgap. These changes, although small, were found consistently on many samples. The observed stabilization of the deep filled states, shown in Figure 3, is, in principle, in agreement with the prototypical case of Figure 2c, because it is the deep states that control the SRV. Thus, the results are essentially in agreement with our qualitative model. Unfortunately, the SPV signal due to these states was only slightly above the noise level. Therefore, a detailed understanding of the surface state changes and a quantitative account of how they produce the SRV increase is not possible here.

At the *n*-CdSe(0001) surface, both DCDC and DHDC adsorption increased the SRV to the upper limit measurable with our setup. Nevertheless, a detailed look at the PL decay curves, shown in Figure 8a, shows that the DHDC decay curve is somewhat slower. Again, this difference, although small, was found consistently. This once again shows that due to the smaller overlap of the DHDC LUMO level with the surface states, its effect is smaller.

We briefly turn to the *n*-InP(001) surface. Here, SPV spectra revealed no surface states, apparently due to an insufficient signal-to-noise ratio, and therefore provided no real way to test the model. However, we found that the DCDC-induced increase in SRV is much greater than that induced by DHDC adsorption, as shown in the PL decay curves of Figure 8b. This suggests that the situation for *n*-InP(001) is similar to that of *n*-CdSe-(0001).

Hybrid Aspects. So far, we have only discussed cases where one type of surface state dominated, so that the extreme cases depicted in Figure 2 could be compared with experiment. However, it is clear that hybrid cases may arise. An obvious example is that if both shallow states and deep states are present, one expects molecular adsorption to induce changes in both V_s and SRV. The relative weight of these changes depends on the relative density of the various surface state populations.

A case in point is the type II *n*-CdTe(100) surface. According to Table 1, its SRV is much larger than that of the type I surfaces. This suggests that the type II surface has a much larger density of effective recombination centers, i.e., of deep states. We therefore expect that whereas filled shallow states would still be pushed inside the VB, more of the filled deep states will remain within the band gap and the reduction in V_s will not be as large as that found at type I surfaces. This is indeed observed experimentally.

For a different example, we take another look at the *n*-GaAs-(100) surface. According to Table 1, the SRV was slightly increased upon DCDC adsorption. It should be taken into account that in this case the samples used had a high doping level (above 10^{18} cm^{-3}). Therefore, the width of the surface depletion width was smaller than the absorption length of the 870 nm photons. This causes the PL decay curve to be significantly influenced by bulk recombination. As the latter clearly does not change upon surface treatment, it is quite possible that the real increase in SRV was somewhat higher than that given in Table 1. Indeed, a somewhat larger SRV increase was observed at GaAs surfaces of lower-doped samples. This shows that whereas the dominating effect at the *n*-GaAs-(100) surface was a decrease in band bending, as discussed above, some change in the SRV was also present, even though the deep states did not dominate the SPV spectra. Likewise, some DCDC-induced reduction in band bending was observed at the *n*-CdSe surface, even though shallow states did not dominate the SPV spectrum of that surface.

Overview. The different experimental examples given above clearly corroborate our theoretical model, where a similar molecule−surface interaction mechanism induces greatly varying changes in the surface gap state positions, and therefore in band bending and SRV. Generally, the ability of the chemical treatment to modify the electronic properties of the different semiconductor surfaces was found to depend on two important parameters: (i) the molecule's energy level and its energy distance from the interacting surface states and (ii) the energy levels and densities of the interacting surface states. For parameter (i), the smaller this energy distance is, the stronger is the surface−molecule coupling and the larger are the induced changes in surface electronic properties. Here, larger changes were consistently observed with DCDC, the LUMO of which lies lower in energy than that of DHDC and therefore interacts more effectively with the pertinent surface states. For parameter (ii), in general, in samples where the dominating surface states are close to the bands (CdTe, GaAs) the interaction's main effect is the reduction of the band bending. In samples where the dominating surface states are close to midgap (CdSe, InP), the interaction's main effect is the modification of the SRV.

Examining these parameters, a simple guideline for the passivation of semiconductor surfaces with molecular treatments emerges. One must start by mapping the surface state energies relative to the band edges and then choose a molecule with known frontier orbital energies that are close to the dominant surface states. The wide variety of organic molecules and the ability to tune their LUMO energy levels greatly increases the probability of finding molecules appropriate to the fine-tuning of widely differing semiconductor surfaces.

V. Conclusions

In this paper, we have studied the surface electronic effects induced by molecular treatments of semiconductors, using a combination of surface photovoltage and photoluminescence measurements. These changes were explained by a surface state-molecule, HOMO−LUMO like interaction, where either the surface states or the molecular level may play the role of the HOMO level, depending on their relative energy position and their population. It was shown, both theoretically and experimentally, that despite the consistent interaction mechanism, its electronic consequences might vary greatly, depending on the surface state energy position and the strength of the molecule-surface state coupling. Furthermore, we demonstrated that the efficacy of a given molecular treatment could be predicted qualitatively, based on the surface state and LUMO energy levels. The present findings can contribute to our understanding of molecule-surface interactions. They can also be used as guidelines for organic molecule-aided surface engineering of semiconductors and potentially, in the farther future, that of molecule-based electronic devices.

Acknowledgment. We thank Dr. Vera Lyahovitskaya for doping the CdTe crystals, Tamar Moav and Rachel Lazar for preparation of the dicarboxylic acids, Dori Gal for help in the SPS measurements, and Dr. Dave Waldeck (University of Pittsburgh) for helpful discussions. We thank a reviewer for bringing up the point referred to in footnote 28. This work was supported in part by the US−Israel Binational Science Foundation, Jerusalem, Israel. D.C. and A.S. acknowledge partial support from the Israel Ministry of Science's Tashtyoth program. A.B.E. and J.K.L. acknowledge the National Science Foundation for support.

Supporting Information Available: FTIR dta on the adsorption of DCDC on GaAs, CdTe, and CdSe crystals and FTIR spectra of DCDC (PDF). This material is available free of charge via the Internet at http://pubs.acs.org.

JA9906150